Redox Biology 15 (2018) 86–96

Contents lists available at ScienceDirect

Redox Biology

journal homepage: www.elsevier.com/locate/redox

Research Paper

Synergistic interaction of fatty acids and oxysterols impairs mitochondrial function and limits liver adaptation during nafld progression

Francesco Bellanti[a], Rosanna Villani[a], Rosanna Tamborra[a], Maria Blonda[a,b], Giuseppina Iannelli[a], Giorgia di Bello[a], Antonio Facciorusso[a], Giuseppe Poli[c], Luigi Iuliano[d], Carlo Avolio[b], Gianluigi Vendemiale[a], Gaetano Serviddio[a,*]

[a] C.U.R.E. University Centre for Liver Disease Research and Treatment, Institute of Internal Medicine, Department of Medical and Surgical Sciences, University of Foggia, 71122 Foggia, Italy
[b] Institute of Neurology, Department of Medical and Surgical Sciences, University of Foggia, 71122 Foggia, Italy
[c] Department of Clinical and Biological Sciences, University of Torino at San Luigi Gonzaga Hospital, 10043 Orbassano, Torino, Italy
[d] Laboratory of Vascular Biology and Mass Spectrometry, Department of Medico-Surgical Sciences and Biotechnologies, Sapienza University of Rome, 04100 Latina, Italy

ARTICLE INFO

Keywords:
Oxysterols
Non-alcoholic fatty liver disease
Mitochondria
Cholesterol excess
Fatty acids

ABSTRACT

The complete mechanism accounting for the progression from simple steatosis to steatohepatitis in nonalcoholic fatty liver disease (NAFLD) has not been elucidated. Lipotoxicity refers to cellular injury caused by hepatic free fatty acids (FFAs) and cholesterol accumulation. Excess cholesterol autoxidizes to oxysterols during oxidative stress conditions. We hypothesize that interaction of FAs and cholesterol derivatives may primarily impair mitochondrial function and affect biogenesis adaptation during NAFLD progression. We demonstrated that the accumulation of specific non-enzymatic oxysterols in the liver of animals fed high-fat + high-cholesterol diet induces mitochondrial damage and depletion of proteins of the respiratory chain complexes. When tested *in vitro*, 5α-cholestane-3β,5,6β-triol (triol) combined to FFAs was able to reduce respiration in isolated liver mitochondria, induced apoptosis in primary hepatocytes, and down-regulated transcription factors involved in mitochondrial biogenesis. Finally, a lower protein content in the mitochondrial respiratory chain complexes was observed in human non-alcoholic steatohepatitis. In conclusion, hepatic accumulation of FFAs and non-enzymatic oxysterols synergistically facilitates development and progression of NAFLD by impairing mitochondrial function, energy balance and biogenesis adaptation to chronic injury.

1. Introduction

Nonalcoholic fatty liver disease (NAFLD), the most common liver pathology in the Western world [1], may clinically present with a heterogeneity of conditions ranging from benign steatosis (NAFL) to steatohepatitis (NASH) – the more progressive form of the disease [2] – and to cirrhosis. The mechanisms underlying the transformation from non inflamed to inflamed fatty liver are not completely elucidated, even though lipid metabolism alterations, mitochondrial dysfunction, inflammation and oxidative stress are suggested to play a significant role [3–6].

Accumulating lipids in hepatocytes may be vulnerable to free radical-induced peroxidation. Lipid peroxides exert toxic effects on the mitochondrial DNA (mtDNA), RNA and proteins of the respiratory chain, leading to mitochondrial dysfunction [7].

Lipotoxicity refers to cellular injury caused by excess of free fatty acids (FFAs) and related-lipid metabolites [8]. Excess cholesterol can lead to dysregulation of cholesterol metabolism, which is considered an underlying pathology in the development of many metabolic diseases [9]. Loading mitochondria with free cholesterol sensitizes hepatic cells to inflammatory mediators such as Tumor Necrosis Factor (TNF) and cell-surface Fas receptor (Fas), which may precipitate steatohepatitis

Abbreviations: NAFLD, non-alcoholic fatty liver disease; NAFL, non-alcoholic fatty liver; NASH, non-alcoholic steatohepatitis; mtDNA, mitochondrial DNA; FFAs, free fatty acids; TNF, tumor necrosis factor; CTRL, control; HF, high-fat; HF + HCh, high-fat + high-cholesterol; 7β-OHC, 7β-hydroxycholesterol; 5β, 6β-epoxy, 5β,6β-epoxycholesterol; 5α, 6α-epoxy, 5α,6α-epoxycholesterol; triol, 5α-cholestane-3β,5,6β-triol; 7KC, 7-ketocholesterol; 6-oxo, 6-oxo-cholestan-3β,5α-diol; PA, palmitic acid; OA, oleic acid; $\Delta\psi_{;}$, mitochondrial membrane potential; CT, threshold cycle; BN-PAGE, Blue Native bidimensional polyacrylamide gel electrophoresis; SDM, standard deviation of the mean; ANOVA, analysis of variance; MMP, mitochondrial membrane potential; UCP2, uncoupling protein 2; PGC1α, peroxisome proliferator-activated receptor-γ coactivator 1 α; TFAM, mitochondrial transcription factor A, NRF1, nuclear respiratory factor 1; CYPs, cytochromes P450

* Corresponding author.
E-mail address: gaetano.serviddio@unifg.it (G. Serviddio).

https://doi.org/10.1016/j.redox.2017.11.016
Received 29 September 2017; Received in revised form 7 November 2017; Accepted 18 November 2017
Available online 05 December 2017

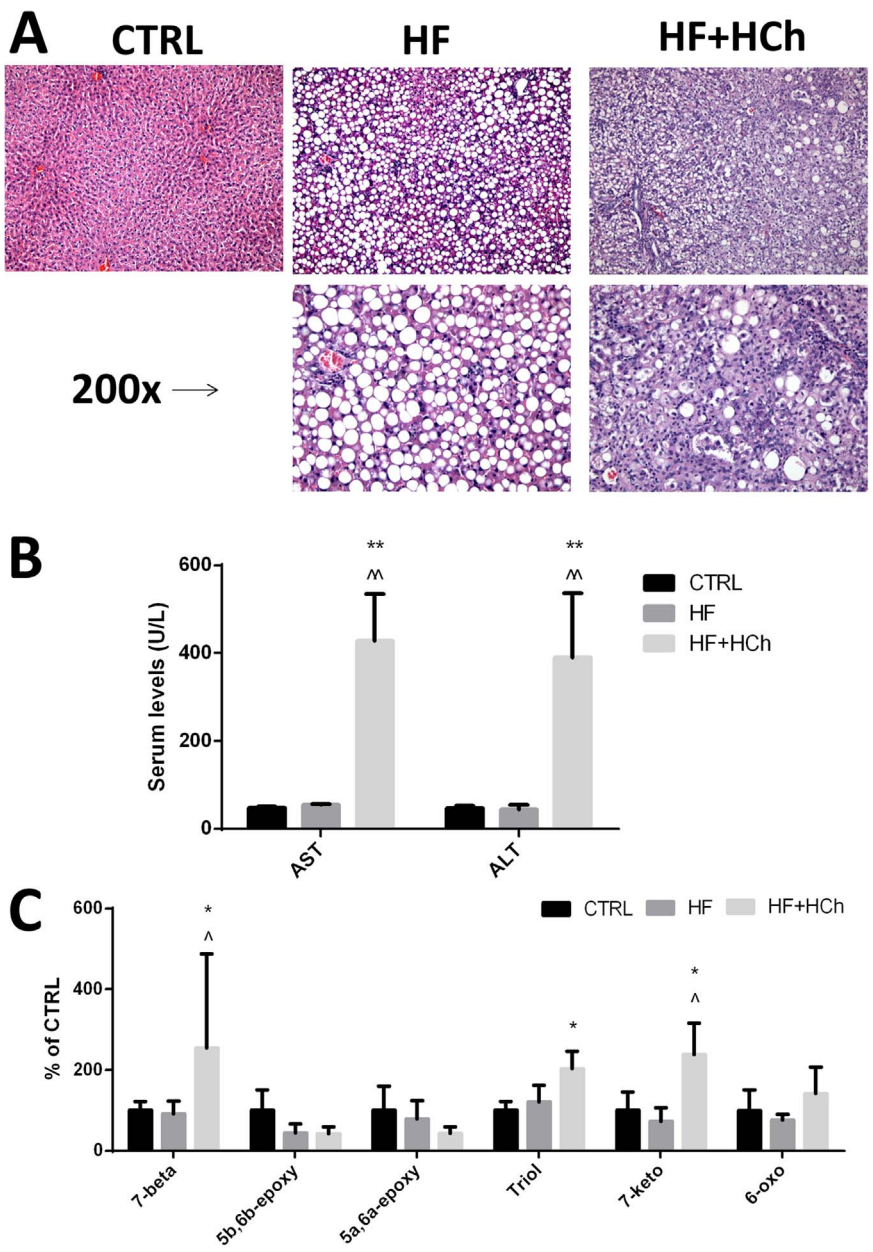

Fig. 1. Increased non-enzymatic oxysterol levels in the liver of HF + HCh-induced NASH. (A) Histological analysis of representative liver samples from rats fed a standard (CTRL), high-fat (HF) or high-fat + high-cholesterol (HF + HCh) diet, stained with Haematoxilin & Eosin (magnification 100x and 200x). (B) Serum levels of aspartate aminotransferase (AST) and alanine aminotransferase (ALT) in all the animal groups studied. (C) Hepatic levels of the non-enzymatic oxysterols measured by mass spectrometry in all the groups studied. Data are expressed as mean ± SDM of five consecutive experiments. Statistical differences were assessed by one-way ANOVA and Tukey-Kramer as post-hoc test (* = $p < 0.05$ vs CTRL; ** = $p < 0.01$ vs CTRL; ^ = $p < 0.05$ vs HF; ^^ = $p < 0.01$ vs HF). 7 beta, 7β-hydroxycholesterol; 5b,6b-epoxy, 5β,6β-epoxycholesterol; 5a,6a-epoxy, 5α,6α-epoxycholesterol; triol, 5α-cholestane-3β,5,6β-triol; 7-keto, 7-ketocholesterol; 6-oxo, 6-oxo-cholestan-3β,5α-diol.

Table 1
Kleiner scoring system applied to liver samples from rats fed a standard (CTRL), high-fat (HF) or high-fat + high-cholesterol (HF + HC) diet.

	Steatosis	Ballooning	Lobular Inflammation	Activity Score	Indication
CTRL	0	0	0	0	Normal
HF	3	0	1	4	NAFL
HF + HCh	2	2	2	6	NASH

[10]. Free cholesterol accumulation in oxidative settings may promote its oxidization with final production of oxysterols that are involved in NAFLD damage [11,12]. Dietary fat and cholesterol induce the metabolic and hepatic features of NASH in mice only when acting synergistically but not when administered alone [13]. We have previously shown that the significant change in fatty acid and oxysterols profile induced by a dietary combination of high fat and high cholesterol accounts for liver injury, allowing the generation of interesting hypotheses on the role of interaction of lipid and cholesterol metabolites in the pathogenesis of NAFLD progression [14].

In the present study, after a lipidomic analysis of hepatic non-enzymatic oxysterols in animals fed high-fat or high-fat + high-cholesterol diet, we analyzed mitochondrial function, biogenesis and mitochondrial respiratory chain proteins, and we demonstrated a significant impairment in the respiratory chain and energy homeostasis secondary to depletion of specific respiratory chain complexes. The analysis of mitochondrial biogenesis signaling revealed that FFAs and non-enzymatic oxysterols synergistically interact and limit the adaptive response of liver cells to chronic lipid accumulation, promoting transition from steatosis to steatohepatitis. The observations were then confirmed in human NASH.

2. Materials and methods

Further details are provided in the Supporting Information.

Table 2
Respiratory activity, Respiratory Control Index (RCI) and Membrane Potential (MMP) in isolated liver mitochondria from rats fed the standard (CTRL), high-fat (HF) or high-fat + high-cholesterol (HF + HC) diets for 6 weeks. Data are expressed as mean ± SDM of five consecutive experiments. Statistical differences were assessed by one-way ANOVA and Tukey-Kramer as post-hoc test (* = $p < 0.05$ vs CTRL, ^ = $p < 0.05$ vs HF).

		CTRL	HF	HF + HCh
Complex I				
	State 4 (nmolO_2/min/mg)	2.5 ± 0.6	4.1 ± 1.3	4.4 ± 3.9
	State 3 (nmolO_2/min/mg)	13.5 ± 2.3	13.3 ± 4.1	**9.2 ± 5.6***
	RCI	5.5 ± 0.4	3.9 ± 0.8	**2.5 ± 2.2***
	Uncoupled/State 3	0.8 ± 0.1	1.0 ± 0.1	1.0 ± 0.1
Complex II				
	State 4 (nmolO_2/min/mg)	14.3 ± 7.1	20.2 ± 3.9	**41.4 ± 22.6*,^**
	State 3 (nmolO_2/min/mg)	31.8 ± 16.3	40.1 ± 11.4	**68.8 ± 23.7***
	RCI	2.2 ± 0.1	2.0 ± 0.7	1.77 ± 0.30
	Uncoupled/State 3	1.2 ± 0.2	1.2 ± 1.0	1.4 ± 0.1
Complex IV				
	State 4 (nmolO_2/min/mg)	59.3 ± 24.6	40.8 ± 10.8	78.9 ± 36.1
	Uncoupled State (nmolO_2/min/mg)	85.2 ± 30.4	80.3 ± 15.8	99.3 ± 34.8
MMP (mV)		172 ± 2	**156 ± 3***	**149 ± 6***

2.1. Animals and experimental design

Male Wistar rats (Harlan, San Pietro al Natisone, Italy) were divided into the following 3 groups: CTRL, control rats given a standard chow; HF, rats given a high-fat diet (60% cocoa butter); HF + HCh, rats fed a high-fat and high-cholesterol diet (60% cocoa butter + 1.25% cholesterol). The compositions of the diets has been previously shown in [15].

2.1.1. Human study

Liver specimens were obtained during non-hepatic abdominal surgery from 18 consecutive patients (10 NASH and 8 steatosis, according to liver histology) and 8 healthy subjects undergoing laparoscopic cholecystectomy. All subjects included in the study were negative for viral hepatitis infection, liver autoimmune or metabolic disorders and were not under treatment with hepatotoxic drugs. All patients gave written informed consent to the study, which was conducted according to the Declaration of Helsinki.

2.1.2. Oxysterols measurement

For cholesterol oxidation markers, we measured in liver samples the oxysterols generated *via* a free radical–mediated mechanism (7β-hydroxycholesterol, 7β-OHC; 5β,6β-epoxycholesterol, 5β,6β-epoxy; 5α,6α-epoxycholesterol, 5α,6α-epoxy; 5α-cholestane-3β,5,6β-triol, triol; 7-ketocholesterol, 7KC; 6-oxo-cholestan-3β,5α-diol, 6-oxo) by mass spectrometry with isotope-dilution methods, as previously reported [14].

2.1.3. Rat hepatocytes isolation, culture and treatment

Hepatocytes were isolated from non-treated animals using a modified collagenase perfusion technique as described previously [16]. Cells were treated for 24 h with 7β-OHC, 7-KC or triol to give a final concentration of 10^{-6}, 10^{-5}, 10^{-4}, and 10^{-3} M. 7β-OHC, 7-KC and Triol were dissolved in ethanol for delivery to cells and the final concentration of ethanol in the cultures did not exceed 0.1% (v/v). Equivalent quantities of ethanol were added to control cells. The treatment with oxysterols was also performed in the presence of palmitic (PA) or oleic acid (OA), at titrated concentrations. Cellular survival was determined by the microculture tetrazolium assay [17], while apoptosis was analyzed using the annexin V-fluorescein isothiocyanate apoptosis detection kit (Beckman Coulter, Milan, Italy).

2.1.4. Oxygraphic measurements

Respiratory rates were measured in isolated hepatocytes as described [18]. Freshly prepared liver mitochondria were assayed for oxygen consumption as previously reported [19]. Mitochondrial membrane potential (Δψ) and proton leak analysis were measured as previously reported [19].

2.1.5. Evaluation of F_OF_1ATPase activity and tissue ATP content

F_OF_1ATPase activity was measured following ATP hydrolysis with an ATP-regenerating system coupled to NADPH oxidation [20]. The hepatic ATP concentration was assessed by bioluminescence (Enliten ATP assay kit - Promega Corporation, Madison, WI, USA) according to the method of Yang [21].

2.1.6. Measurement of mitochondrial H_2O_2 production

The rate of peroxide production was determined in isolated liver mitochondria following the oxidation of Amplex Red by horseradish peroxidase as previously reported [19].

2.1.7. q-PCR array of mitochondrial energy metabolism – related genes

20 ng cDNA was loaded into each well in RT2 Profiler 96-well PCR array plates (PARN-008Z, QIAGEN, Valencia CA). The median cycle threshold value (CT) was uploaded onto the SABioscience website (http://pcrdataanalysis.sabiosciences.com/pcr/arrayanalysis.php) and the fold change of each gene expression was calculated using the provided software according to manufacturer's instruction.

2.1.8. Gene expression analysis by real-time RT-PCR

Real-time RT-PCR was performed on RNA extracted from human liver tissue or rat primary hepatocytes, using SYBR Green I assay in Bio-Rad iCycler detection system as previously reported [19]. A PCR master mix containing the specific primers shown in Supplementary Table 1 was used. The threshold cycle (CT) was determined, and the relative gene expression subsequently was calculated as follows: fold change = $2^{-\Delta(\Delta CT)}$, where ΔCT = CT − CT target housekeeping and Δ(ΔCT) = ΔCT – ΔCT treated control.

2.1.9. Blue Native bidimensional polyacrylamide gel electrophoresis (BN-PAGE)

BN-PAGE was performed on human liver mitochondria proteins as described [22]. First, solubilized samples were stained with a charged (Coomassie) dye. The intact mitochondrial complexes were then separated by electrophoresis based upon how much dye was bound, which is proportional to their size. After this first dimension gel, which was run in a 5–12% acrylamide gradient, a lane was cut out and placed on a glass plate for incubation with lysis buffer at room temperature. The protein components of the resolved complexes were separated in a second dimension after soaking the gel in denaturing SDS buffer. For the detection of all five OXPHOS complexes simultaneously a mix of monoclonal antibodies was used (MitoScience MS603 kit, AbCam, Oregon, USA).

2.1.10. Statistical analysis

The data were normally distributed and were expressed as mean ± standard deviation of the mean (SDM). Differences between the groups were determined by one-way analysis of variance (ANOVA) with Tukey-Kramer as *post hoc* test. Statistical significance was accepted when $P < 0.05$. The GraphPad Prism 6.0 Software was used to perform the analysis.

3. Results

3.1. Combination diet (HF + HCh) increases non-enzymatic oxysterol level in NASH liver

Rats fed high-fat diet (HF) for 6 weeks showed severe liver steatosis

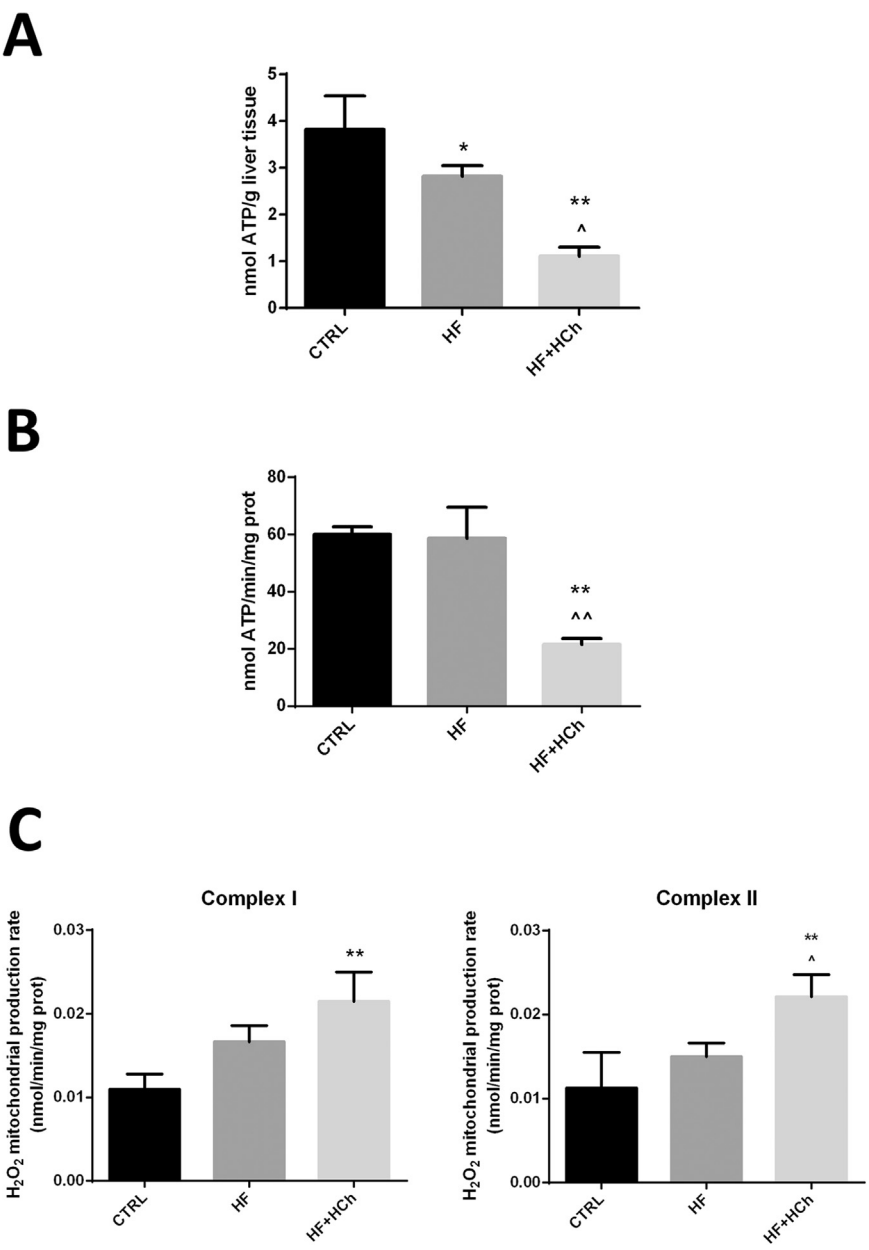

Fig. 2. Hepatic ATP homeostasis and mitochondrial H_2O_2 production rate impairment in HF + HCh-induced NASH. (A) Hepatic ATP content in rats fed a standard (CTRL), high-fat (HF) or high-fat + high-cholesterol (HF + HCh) diet for 6 weeks. (B) Complex V (ATPase) activity in all the groups studied. (C) hydrogen peroxide production rate in liver mitochondria from all the groups studied, using glutamate + malate (Complex I) or succinate in the presence of rotenone (Complex II) as oxidative substrates. Data are expressed as mean ± SDM of five consecutive experiments. Statistical differences were assessed by one-way ANOVA and Tukey-Kramer as post-hoc test. (* = $p < 0.05$ vs CTRL; ** = $p < 0.01$ vs CTRL; ^ = $p < 0.05$ vs HF; ^^ = $p < 0.01$ vs HF).

but mild lobular inflammation; on the other hand, animals fed the high-fat + high-cholesterol diet (HF + HCh) exhibited a severe liver damage characterized by macrovesicular steatosis, hepatocytes ballooning and diffused lobular infiltration, as well as increased serum aminotransferase levels, suggestive of NASH (Fig. 1A and B, Table 1).

The lipidomic analysis of non-enzymatic oxysterols in rat liver revealed a significant increase of 7β-hydroxycholesterol (7β-OHC), 7-ketocholesterol (7-KC) and 5α-cholestane-3β,5,6β-triol (Triol) in the HF + HCh livers, as compared to the CTRL and HF groups (Fig. 1C).

3.2. Mitochondrial function, ATP homeostasis and biogenesis are severely impaired in livers feeding HF and HC combination diet

Freshly isolated mitochondria were analyzed in terms of oxygen consumption rate, mitochondrial membrane potential (MMP), hydrogen peroxide production rate, ATP homeostasis and proton leak kinetics.

Oxygen uptake was impaired by the mitochondrial Complex I (while it was enhanced by the Complex II) in the HF + HCh group as compared to CTRL rats; however, MMP was reduced both in the HF and in the HF + HCh group (Table 2).

We then analyzed the hepatic ATP homeostasis and observed that both diets induced a reduction in the liver ATP content when compared to CTRL (Fig. 2A). To determine whether the reduction of ATP was dependent on an impairment in mitochondrial ATP synthesis, the enzymatic activity of Complex V (ATP-synthase) was measured and we observed a severe reduction in animals fed the HF + HCh but not the HF diet (Fig. 2B).

The dissipation of MMP through the mitochondrial membranes (proton leak) is a well-established hallmark of mitochondrial dysfunction in NAFLD [23]. Mitochondria proton leak was observed in both the HF and the HF + HCh livers as compared to CTRL (Fig. 3A), and was associated with increased Uncoupling Protein 2 (UCP2) expression (Fig. 3B-D).

Impaired mitochondria produce free radicals, which were quantified by measuring the hydrogen peroxide (H_2O_2) production rate using pyruvate/malate or succinate as mitochondrial substrates. The rate of H_2O_2 synthesis was not changed in the HF group with respect to CTRL;

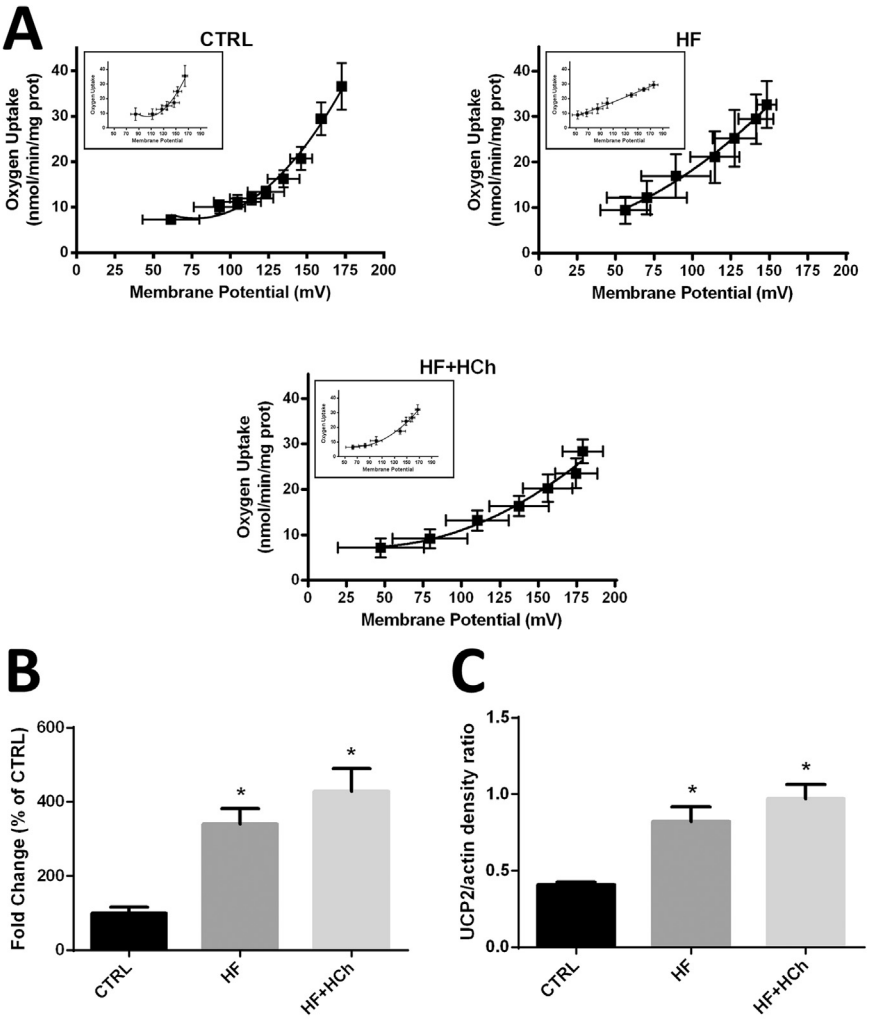

Fig. 3. Increased mitochondrial uncoupling and UCP2 expression in NAFLD. (A) Proton leak kinetics in mitochondria isolated from rats fed a standard (CTRL), high-fat (HF) or high-fat + high-cholesterol (HF + HCh) diet for 6 weeks. The membrane potential dependence of the proton leak rate was determined in mitochondria oxidizing succinate (10 mM) in the presence of rotenone. Oligomycin was added to inhibit ATP synthase activity. The small figures show the proton permeability obtained after mitochondrial pre-incubation with the uncoupling proteins'inhibitor guanosine diposphate (GDP). The proton permeability was prevented by GDP in HF + HCh, but not in HF. (B) Gene expression of the Uncoupling Protein 2 (UCP2) measured by real time rt-PCR in the liver of all groups studied. (C) and (D) Densitometric analysis and representative blot of UCP2 immunoprecipitated in liver mitochondria proteins from all the groups studied. Data are expressed as mean ± SDM of five consecutive experiments. Statistical differences were assessed by one-way ANOVA and Tukey-Kramer as post-hoc test.

on the contrast, the HF + HCh group showed a higher rate of mitochondrial ROS production (Fig. 2C).

Taken together, these data show that the addition of cholesterol to a high fat diet induces a significant change in the non-enzymatic oxysterol profile that in turn induces a severe hepatic impairment of mitochondrial function.

A Mitochondrial Energy Metabolism PCR Array was used to determine the expression profile of 84 key genes involved in mitochondrial respiration, including those encoding components of the electron transport chain and oxidative phosphorylation complexes.

As shown in Table 3A, the HF group presented the up-regulation of Cox15, Bcs1L and Atp4a genes as compared to CTRL. On the contrast, several genes encoding for subunits of mitochondrial Complex I, IV and V were down-regulated in the HF + HCh (Table 3B), suggesting a severe reduction of respiratory chain proteins.

3.3. Non-enzymatic oxysterols synergistically interact with FFAs and impair mitochondrial function and biogenesis in vitro

To study a possible synergistic interaction between specific oxysterols and fatty acids in the induction of liver injury, different combinations of free fatty acids with 7β-OHC, 7-KC or triol were tested *in vitro*. Rat primary hepatocytes were incubated with 50 μM palmitic acid (PA) as saturated fatty acid, and 2 mM oleic acid (OA) as unsaturated fatty acid for 24 h. The addition of Triol to PA/OA significantly reduced the viability of the primary hepatocytes at concentrations of 10 or 100 μM (Fig. 4A); however, the same concentration of 7β-OHC or 7-KC did not induce any significant effect (supplementary material, Fig. S3A and B). By flow cytometry we verified that the combination of the lowest concentration of Triol (10 μM) + PA/OA induced hepatocellular necrosis (7-AAD positive cells) rather than apoptosis (annexin V-stained cells), while minimal effects were observed using Triol or PA/OA alone (Fig. 4B).

The effects of 7β-OHC, 7-KC and triol were also tested on the

Table 3
List of the genes up- or down-regulated (> 2 fold) in the HF (A) and HF + HC (B) groups with respect to CTRL. Changes in gene expression between groups were evaluated using RT2 Profiler 96-well PCR array plates. Data analysis was done by the 2-DDCt method on the manufacturer's Web portal (http://www.SABiosciences.com/pcrarraydataanalysis.php), (QIAGEN, CA, USA).

RefSeq	Symbol	Description	Fold Change
A			
NM_001033699	Cox15	Cytochrome c oxidase assembly protein (yeast)	2,1936
NM_01007666	Bcs1l	BCS1-like (yeast)	4
NM_012509	Atp4a	ATPase, H^+/K^+ exchanging, alpha polypeptide	2,1936
B			
NM_133517	Atp12a	ATPase, H^+/K^+ transporting, alpha polypeptide	−3,4983
NM_012510	Atp4b	ATPase, H^+/K^+ exchanging, beta polypeptide	−3,4983
NM_023093	Atp5a1	ATP synthase, mitochondrial F_1 complex, alpha subunit 1	−2,0093
NM_134364	Atp5b	ATP synthase, mitochondrial F_1 complex, beta polypeptide	−2,4172
NM_053825	Atp5c1	ATP synthase, mitochondrial F_1 complex, gamma polypeptide 1	−2,1535
NM_080481	Atp5i	ATP synthase, mitochondrial F_0 complex, subunit e	−3,4983
NM_053602	Atp5j	ATP synthase, mitochondrial F_0 complex, subunit F6	−2,1043
NM_212516	Atp5l	ATP synthase, mitochondrial F_0 complex, subunit G	−2,0093
NM_031785	Atp6ap1	ATPase, H^+ transporting, lysosomal accessory protein 1	−2,1535
NM_001014199	Atp6v1c2	ATPase, lysosomal V_1 subunit C2	−3,4983
NM_001108979	Atp6v1e2	ATPase, lysosomal V_1 subunit E2	−3,4983
NM_01007666	Bcs1l	BCS1-like (yeast)	−2,1043
NM_017202	Cox4i1	Cytochrome c oxidase subunit IV isoform 1	−2,4172
NM_145783	Cox5a	Cytochrome c oxidase, subunit Va	−2,1043
NM_012812	Cox6a2	Cytochrome c oxidase subunit VIa polypeptide 2	−3,4184
NM_019360	Cox6c	Cytochrome c oxidase, subunit Vic	−3,1895
NM_022503	Cox7a2	Cytochrome c oxidase subunit VIIa polypeptide 2	−2,2038
NM_182819	Cox7b	Cytochrome c oxidase subunit VIIb	−2,1535
NM_183055	Cox8c	Cytochrome c oxidase, subunit VIIIc	−3,4983
NM_001009706	Lhpp	Phospholys phosphohistidine inorganic pyrophosp phosphatase	−4,9474
NM_001108813	Ndufa1	NADH dehydrogenase 1 alpha subcomplex, 1	−3,0455
NM_212517	Ndufa11	NADH dehydrogenase 1 alpha subcomplex 11	−2,0562
NM_001106153	Ndufa2	NADH dehydrogenase 1 alpha subcomplex, 2	−2308
NM_001106646	Ndufb6	NADH dehydrogenase 1 beta subcomplex, 6	−2,0093
NM_001108442	Ndufb7	NADH dehydrogenase 1 beta subcomplex, 7	−2,2553
NM_001127294	Ndufb9	NADH dehydrogenase 1 beta subcomplex, 9	−2,5907
NM_001011907	Ndufs2	NADH dehydrogenase Fe-S protein 2	−3,1895
NM_001106489	Ndufs3	NADH dehydrogenase Fe-S protein 3	−2,2038
NM_001100539	Sdhb	Succinate dehydrogenase complex, subunit B, iron sulfur	−2,2553
NM_198788	Sdhd	Succinate dehydrogenase complex, subunit D	−2,0093
NM_133418	Slc25a10	Solute carrier family 25, member 10	−2,2553
NM_001047880	Slc25a15	Solute carrier family 25, member 15	−3,3404
NM_012682	Ucp1	Uncoupling protein 1	−3,4983
NM_013167	Ucp3	Uncoupling protein 3	−3,4983
NM_001025134	Uqcrq	Ubiquinol-cytochrome c reductase, complex III subunit VII	−3,4983

mitochondrial bioenergetics; to this, the oxygen consumption was measured on both isolated liver mitochondria and intact primary hepatocytes. No toxic effect was observed with 7β-OHC or 7-KC (supplementary material, Fig. S4); on the contrary, a dose-dependent reduction of mitochondrial respiration was reported with Triol (Fig. 5A-C). These data suggest that the combination of Triol + PA/OA induced hepatocyte toxicity *via* mitochondrial bioenergetics impairment.

Peroxisome proliferator-activated receptor-γ coactivator 1 α (PGC1α) and its downstream targets, mitochondrial transcription factor A (TFAM) and nuclear respiratory factor 1 (NRF1) are the master regulator of mitochondrial biogenesis.

Interestingly, we observed that incubation of primary hepatocytes with PA + OA in the presence of triol – but not of 7β-OHC or 7-KC – significantly induced down-regulation of PGC1α, TFAM and NRF1, suggesting a causative role for the combination of free fatty acids and Triol in the mitochondrial biogenesis failure and in mitochondrial dysfunction (Fig. 5D).

3.4. Mitochondrial biogenesis is impaired in NASH patients as compared to simple steatosis and healthy livers

The characteristics of studied population are summarized in the Table S2. NASH showed higher fasting serum triglycerides and cholesterol as compared to healthy and steatosis subjects. Freshly isolated mitochondria from human liver specimens were analyzed by 2D electrophoresis and a reduction of proteins related to Complex I, Complex IV and Complex V was observed only in NASH (Fig. 6A) but not in simple steatosis. We then measured the mRNA expression of master regulators of mitochondrial biogenesis and, very interestingly, we observed a 50% reduction in the expression of PGC-1α in NASH livers together with a slight reduction of TFAM and NRF1 (Fig. 6B). These data suggest that, in humans, during NASH development, a mitochondrial reduction of respiratory chain proteins occurs that is not counterbalanced by activation of mitochondrial biogenesis response.

4. Discussion

The pathogenesis of NAFLD is mostly unclear. Clinicians are daily faced with the difficulty to identify patients progressing from simple steatosis to steatohepatitis, who present with a worse prognosis [24]. One of the burning questions in NAFLD remains which factors act as the driving forces toward a progressive inflammatory disease phenotype. Mitochondrial dysfunction has been suggested to play a significant role in the progression of NAFLD [23]. The present study provides a new insight on the mechanism by which free fatty acids and oxysterols interact and induce NAFLD development and progression through the impairment of mitochondrial function and biogenesis response to chronic liver injury.

The accumulation of toxic lipids causes inflammation in the setting of liver steatosis [25]. Several studies focused on triglyceride

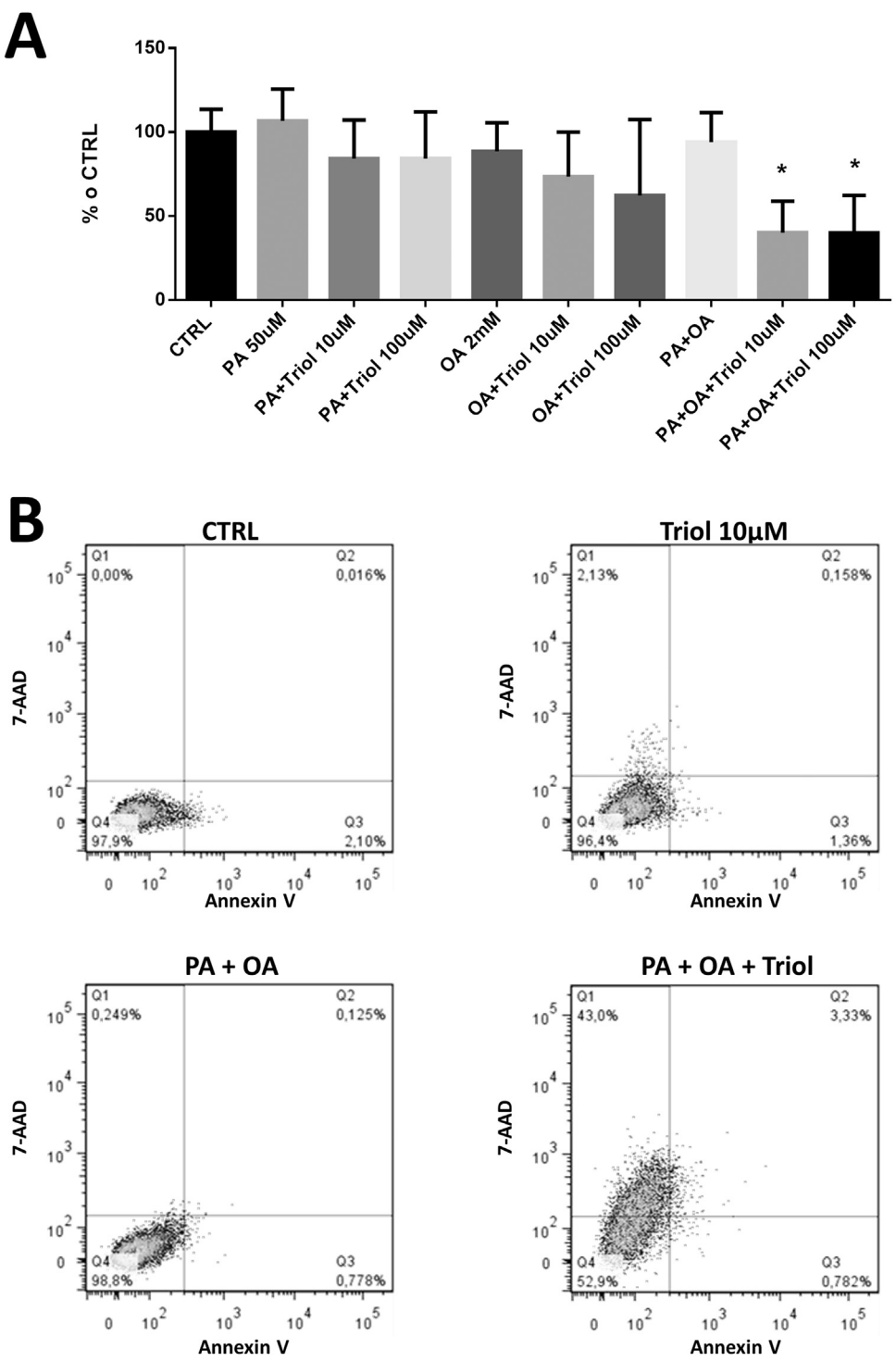

Fig. 4. Co-treating primary hepatocytes with fatty acids and the oxysterol triol induces cell death. (A) Cell viability of rat primary hepatocytes after 24 incubation with palmitic acid (PA) ± oleic acid (OA) ± Triol, assessed by the MTT assay. Data are expressed as mean ± SDM of three consecutive experiments. Statistical differences were assessed by one-way ANOVA and Tukey-Kramer as post-hoc test. (B) Effect of 24 h incubation with Triol 10 µM, palmitic acid 50 µM + oleic acid 2 mM (PA + OA), or palmitic acid 50 µM + oleic acid 2 mM + Triol 10 µM (PA + OA + Triol) on rat primary hepatocytes aptoptosis and necrosis. Apoptotic or necrotic cells were detected by flow cytometry after staining with annexin V and 7-AAD. 50 µM PA and 2 mM OA were chosen as the highes non-toxic concentrations for the induction of cellular steatosis.

accumulation as pathogenic factor [26,27]. Nevertheless, triglyceride storage may protect liver cells from fatty acid-induced apoptotic pathways [28], and blocking triglyceride synthesis leads to less steatosis but more inflammation, oxidative stress and fibrosis [29]. Even though the type of hepatotoxic lipid has not been identified yet, both free fatty acids and cholesterol, especially when accumulated in mitochondria, could lead to liver injury and hepatocellular damage [10,30]. It has been recently demonstrated that administration of peroxidized fatty acids produces a dramatic inflammatory increase into the liver [31]. However, a lipidomic analysis on humans demonstrated that – more than free fatty acids – free cholesterol accumulates in NAFLD [32].

Cholesterol is essential for proper cell function; however, free cholesterol accumulation in an oxidative milieu may promote its oxidization with final production of oxysterols. Cholesterol oxidation involves several mono-oxygenation reactions, which are catalyzed by cytochromes P450 (CYPs). During normal hepatic cholesterol degradation, it can be enzymatically converted to 7α-hydroxycholestrol by 7α-hydroxylase. Other CYPs such as 27-hydroxylase and 4β-hydroxylase catalyze the formation of the mayor oxysterol species 27-hydroxycholesterol and 4β-hydroxycholestrol, respectively. Alternatively, cholesterol can be metabolized by non-enzymatic autoxidation, which leads to the formation of 7-ketocholesterol, 7α-hydroxycholesterol, 7β-hydroxycholesterol, 5,6α-epoxycholesterol and 5,6β-epoxycholesterol. There is increasing interest in the biological activity of oxysterols, not

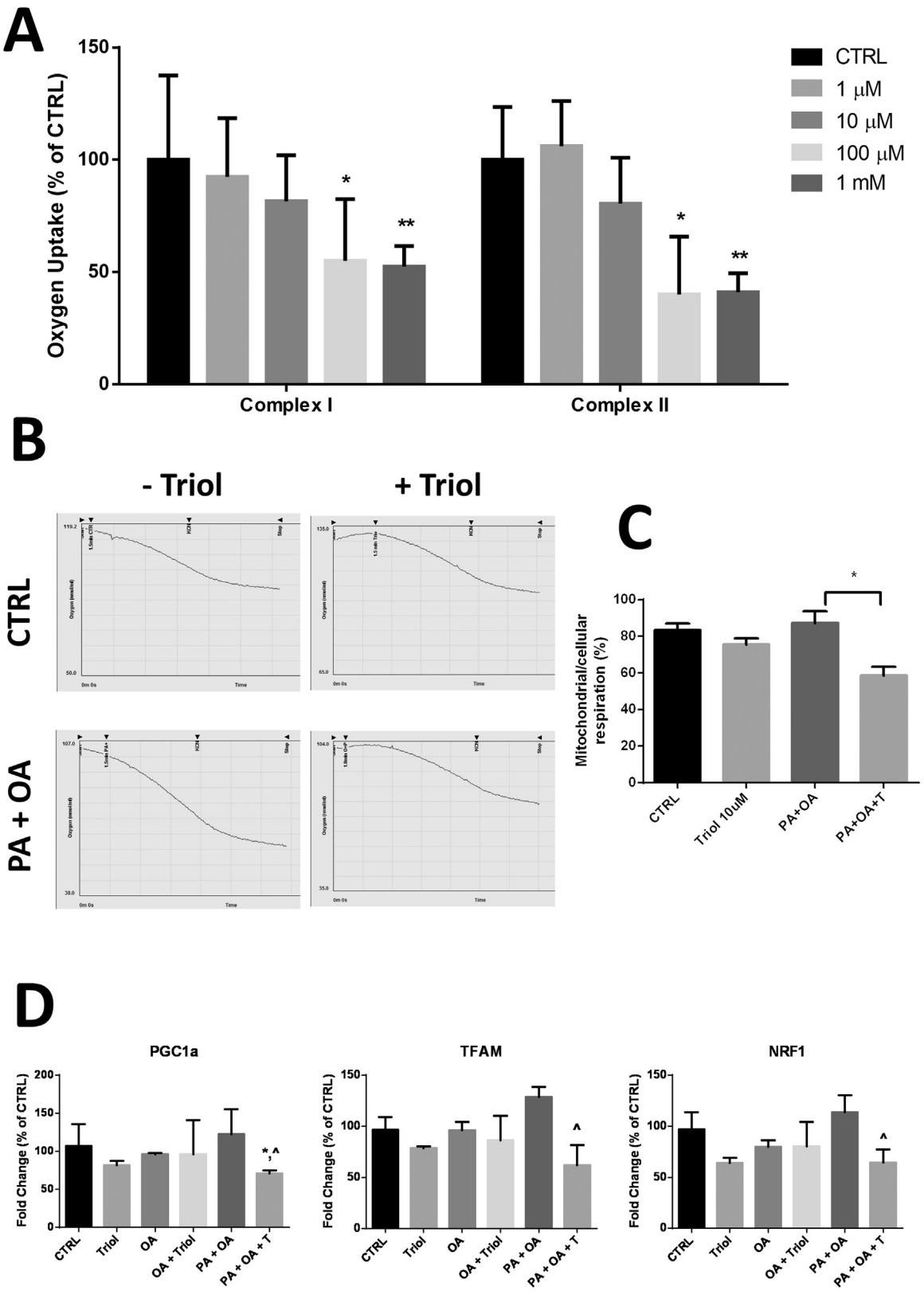

Fig. 5. Mitochondrial function and biogenesis impairment in primary hepatocytes after co-treatment with fatty acids and the oxysterol triol. (A) Oxygen consumption rate of isolated liver mitochondria after incubation with increased concentrations of 5α-cholestane-3β,5,6β-triol (Triol) for 24 h. Mitochondrial respiration was started by pyruvate + malate and glutamate (Complex I) or succinate in the presence of rotenone (Complex II). Data are expressed as mean ± SDM of three consecutive experiments. Statistical differences were assessed by one-way ANOVA and Tukey-Kramer as post-hoc test (* = $p < 0.05$ vs CTRL, ** = $p < 0.01$ vs CTRL). (B) Representative oxygraphic measurement of intact hepatocytes respiration after 24 h incubation with palmitic acid (PA) + oleic acid (OA) ± Triol. (C) Mitochondrial/cellular respiratory rate measured in intact rat primary hepatocytes after 24 h incubation with PA + OA ± Triol. (D) Gene expression of peroxisome proliferator-activated receptor-γ coactivator 1 α (PGC1α), mitochondrial transcription factor A (TFAM) and nuclear respiratory factor 1 (NRF1) measured by real time rt-PCR in the rat primary hepatocytes after 24 h incubation with PA + OA ± Triol. Data are expressed as mean ± SDM of three consecutive experiments. Statistical differences were assessed by one-way ANOVA and Tukey-Kramer as post-hoc test.

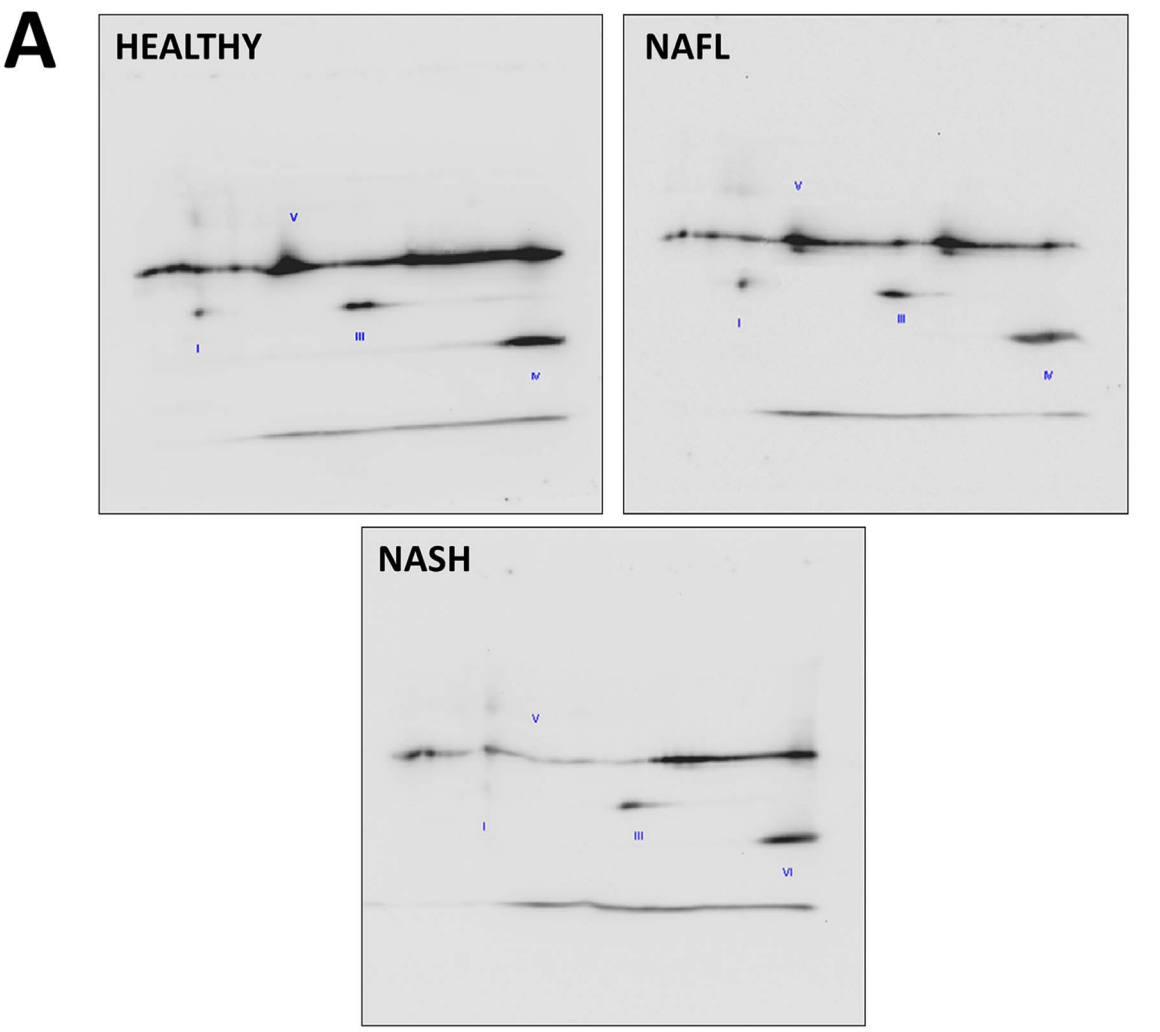

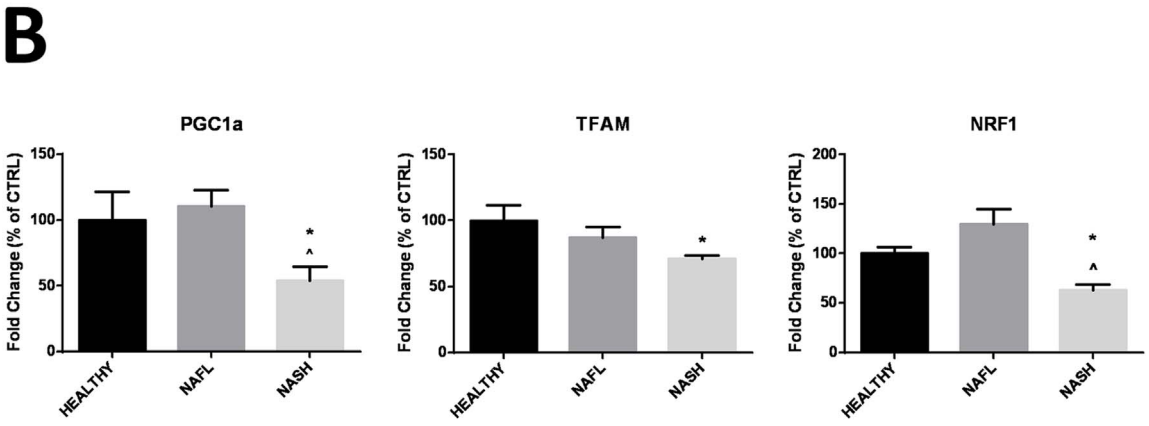

Fig. 6. Reduction of mitochondrial respiratory proteins and master regulators of biogenesis in human NASH. (A) Representative second dimension of a BN-PAGE performed on mitochondrial proteins isolated by the liver of healthy subjects (HEALTHY) and patients affected by simple steatosis (NAFL) or steatohepatitis (NASH). Bands characteristic of individual OXPHOS complexes are recognizable in all three experimental groups. Protein extracts were prepared for each patient, and each individual was assessed separately. Each lane contained 15 μg of mitochondrial protein extract. (B) Gene expression of peroxisome proliferator-activated receptor-γ coactivator 1 α (PGC1α), mitochondrial transcription factor A (TFAM) and nuclear respiratory factor 1 (NRF1) measured by real time rt-PCR in the liver of all patient groups studied. Data are expressed as mean ± SDM of 8+7+10 experiments. Statistical differences were assessed by one-way ANOVA and Tukey-Kramer as post-hoc test.

only because they are non-invasive markers of oxidative stress *in vivo* [33], but also because they may be part of the fine signaling controlling hepatocyte survival in several conditions [34].

We have previously demonstrated that steatohepatitis induced by dietary excess of both fatty acids and cholesterol is associated with a definite oxysterol pattern [14]. In the present study, we have focused on the non-enzymatic oxysterols since the hepatic expression of several enzymes involved in oxysterol generation is reduced in human NASH

[35], and some of enzymatic oxysterols may be even protective, by counteracting the hepatic lipid accumulation and inflammation [36–38]. The intake of oxysterols produced by autoxidation significantly accelerates the development of NAFLD in primates [39]. We show that rats feeding a diet with high fat and high cholesterol develop steatohepatitis and the liver is characterized by high concentrations of non-enzymatic oxysterols such as 7β-hydroxycholesterol (7β-OHC), 7-ketocholesterol (7KC) and triol. This model of liver disease associates with all hallmarks of mitochondrial dysfunction, *i.e.* altered respiration, increased H_2O_2 production, uncoupling and impaired ATP homeostasis.

Several *in vitro* studies demonstrated that 7β-OHC, 7KC and triol are able to induce mitochondrial dysfunction and mitochondria-dependent apoptosis [40–42]. We observed that such oxysterols do not affect cell viability because hepatocytes rapidly metabolize 7KC, the major dietary oxysterol [43,44]. However, triol significantly impaired mitochondrial respiration. Very interestingly, the addition of triol to free fatty acids reduces hepatocytes viability by impairing mitochondrial respiration. Our data show, for the first time, that NASH induced by dietary fatty acid and cholesterol excess associates with mitochondrial dysfunction. Furthermore, when hepatocytes are cultured with a mixture of fatty acids and oxysterols, both mitochondrial respiration and cell viability decrease, suggesting a possible synergic interaction between different lipid species in the pathogenesis of liver cell damage.

A large body of evidence indicates that high-fat diets induce adaptive mechanisms in mitochondrial bioenergetics, such as increased electron transport chain performance and uncoupling [23,45]. On the other side, high-cholesterol diet increases liver mitochondria respiration, uncoupling and induces expression of genes involved in mitochondrial biogenesis [46].

Our data show that combination of HF and HCh diets induce mitochondria dysfunction, alters energy homeostasis and limits the adaptive response to energy demand by impairing mitochondria biogenesis. These finding are strengthened by the bi-dimensional analysis of mitochondrial respiration chain content in human liver, demonstrating that proteins of the Complex I, IV and V are reduced in non-alcoholic steatohepatitis but not in simple steatosis. Moreover, mitochondrial biogenesis response is impaired at the level of PGC-1α, NRF1, and TFAM, which are involved in mtDNA transcription, maintenance, replication and repair [47] in good agreement with previous observations reporting that altered mitochondrial function in human NASH is dependent by defective mitochondrial biogenesis [48].

In conclusion, high-fat diet causes simple steatosis and mild liver injury that do not overwhelm defense response of the liver; on the contrast, the combination of FFAs and cholesterol induces severe inflammation and steatohepatitis and, at cellular level, impairment of mitochondrial function and biogenesis. The pathogenic contribution of cholesterol depends on oxysterols production that are able to disrupt mitochondrial homeostasis, reduce mitochondrial function and energy production and impair the capacity of repair by inhibiting mitochondrial biogenesis. Oxysterols may represent a potential target of novel therapeutic strategy in NAFLD progression.

Acknowledgments/Financial support

Francesco Bellanti is funded by the Development and Cohesion Fund 2007–2013 APQ Research Regione Puglia (FutureInResearch project), and received partial funding by the Italian Society of Internal Medicine (SIMI).

Competing interests

the Authors declare no competing interests.

Appendix A. Supplementary material

Supplementary data associated with this article can be found in the online version at http://dx.doi.org/10.1016/j.redox.2017.11.016.

References

[1] M.M. Smits, G.N. Ioannou, E.J. Boyko, et al., Non-alcoholic fatty liver disease as an independent manifestation of the metabolic syndrome: results of a US national survey in three ethnic groups, J. Gastroenterol. Hepatol. 28 (2013) 664–670.
[2] N. Chalasani, Z. Younossi, J.E. Lavine, et al., The diagnosis and management of non-alcoholic fatty liver disease: practice Guideline by the American Association for the Study of Liver Diseases, American College of Gastroenterology, and the American Gastroenterological Association, Hepatology 55 (2012) 2005–2023.
[3] G. Serviddio, F. Bellanti, G. Vendemiale, et al., Mitochondrial dysfunction in non-alcoholic steatohepatitis, Exp. Rev. Gastroenterol. Hepatol. 5 (2011) 233–244.
[4] G. Serviddio, F. Bellanti, G. Vendemiale, Free radical biology for medicine: learning from nonalcoholic fatty liver disease, Free Radic. Biol. Med. 65C (2013) 952–968.
[5] A. Takaki, D. Kawai, K. Yamamoto, Multiple hits, including oxidative stress, as pathogenesis and treatment target in non-alcoholic steatohepatitis (NASH), Int. J. Mol. Sci. 14 (2013) 20704–20728.
[6] A. Berlanga, E. Guiu-Jurado, J.A. Porras, et al., Molecular pathways in non-alcoholic fatty liver disease, Clin. Exp. Gastroenterol. 7 (2014) 221–239.
[7] P. Schrauwen, V. Schrauwen-Hinderling, J. Hoeks, et al., Mitochondrial dysfunction and lipotoxicity, Biochim. Biophys. Acta 1801 (2010) 266–271.
[8] K. Cusi, The role of adipose tissue and lipotoxicity in the pathogenesis of type 2 diabetes, Curr. Diab Rep. 10 (2010) 306–315.
[9] J.L. Goldstein, M.S. Brown, Regulation of the mevalonate pathway, Nature 343 (1990) 425–430.
[10] M. Mari, F. Caballero, A. Colell, et al., Mitochondrial free cholesterol loading sensitizes to TNF- and Fas-mediated steatohepatitis, Cell Metab. 4 (2006) 185–198.
[11] G. Serviddio, M. Blonda, F. Bellanti, et al., Oxysterols and redox signaling in the pathogenesis of non-alcoholic fatty liver disease, Free Radic. Res. 47 (2013) 881–893.
[12] G. Musso, R. Gambino, M. Cassader, Cholesterol metabolism and the pathogenesis of non-alcoholic steatohepatitis, Prog. Lipid Res. 52 (2013) 175–191.
[13] C. Savard, E.V. Tartaglione, R. Kuver, et al., Synergistic interaction of dietary cholesterol and dietary fat in inducing experimental steatohepatitis, Hepatology 57 (2013) 81–92.
[14] G. Serviddio, F. Bellanti, R. Villani, et al., Effects of dietary fatty acids and cholesterol excess on liver injury: a lipidomic approach, Redox Biol. 9 (2016) 296–305.
[15] N. Matsuzawa, T. Takamura, S. Kurita, et al., Lipid-induced oxidative stress causes steatohepatitis in mice fed an atherogenic diet, Hepatology 46 (2007) 1392–1403.
[16] G. Serviddio, J. Pereda, F.V. Pallardo, et al., Ursodeoxycholic acid protects against secondary biliary cirrhosis in rats by preventing mitochondrial oxidative stress, Hepatology 39 (2004) 711–720.
[17] J.H. Kouadio, T.A. Mobio, I. Baudrimont, et al., Comparative study of cytotoxicity and oxidative stress induced by deoxynivalenol, zearalenone or fumonisin B1 in human intestinal cell line Caco-2, Toxicology 213 (2005) 56–65.
[18] A. Barrientos, In vivo and in organello assessment of OXPHOS activities, Methods 26 (2002) 307–316.
[19] F. Bellanti, A.D. Romano, A.M. Giudetti, et al., Many faces of mitochondrial uncoupling during age: damage or defense? J. Gerontol. A Biol. Sci. Med. Sci. 68 (2013) 892–902.
[20] S. Papa, F. Guerrieri, G. Izzo, Cooperative proton-transfer reactions in the respiratory chain: redox bohr effects, Methods Enzymol. 126 (1986) 331–343.
[21] N.C. Yang, W.M. Ho, Y.H. Chen, et al., A convenient one-step extraction of cellular ATP using boiling water for the luciferin-luciferase assay of ATP, Anal. Biochem. 306 (2002) 323–327.
[22] H. Schagger, Native electrophoresis for isolation of mitochondrial oxidative phosphorylation protein complexes, Methods Enzymol. 260 (1995) 190–202.
[23] G. Serviddio, F. Bellanti, R. Tamborra, et al., Uncoupling protein-2 (UCP2) induces mitochondrial proton leak and increases susceptibility of non-alcoholic steatohepatitis (NASH) liver to ischaemia-reperfusion injury, Gut 57 (2008) 957–965.
[24] M. Ekstedt, L.E. Franzen, U.L. Mathiesen, et al., Long-term follow-up of patients with NAFLD and elevated liver enzymes, Hepatology 44 (2006) 865–873.
[25] B.A. Neuschwander-Tetri, Hepatic lipotoxicity and the pathogenesis of nonalcoholic steatohepatitis: the central role of nontriglyceride fatty acid metabolites, Hepatology 52 (2010) 774–788.
[26] K.L. Donnelly, C.I. Smith, S.J. Schwarzenberg, et al., Sources of fatty acids stored in liver and secreted via lipoproteins in patients with nonalcoholic fatty liver disease, J. Clin. Invest. 115 (2005) 1343–1351.
[27] I.J. Goldberg, H.N. Ginsberg, Ins and outs modulating hepatic triglyceride and development of nonalcoholic fatty liver disease, Gastroenterology 130 (2006) 1343–1346.
[28] L.L. Listenberger, X. Han, S.E. Lewis, et al., Triglyceride accumulation protects against fatty acid-induced lipotoxicity, Proc. Natl. Acad. Sci. USA 100 (2003) 3077–3082.
[29] K. Yamaguchi, L. Yang, S. McCall, et al., Inhibiting triglyceride synthesis improves hepatic steatosis but exacerbates liver damage and fibrosis in obese mice with nonalcoholic steatohepatitis, Hepatology 45 (2007) 1366–1374.
[30] A.E. Feldstein, N.W. Werneburg, A. Canbay, et al., Free fatty acids promote hepatic lipotoxicity by stimulating TNF-alpha expression via a lysosomal pathway, Hepatology 40 (2004) 185–194.
[31] T. Bohm, H. Berger, M. Nejabat, et al., Food-derived peroxidized fatty acids may trigger hepatic inflammation: a novel hypothesis to explain steatohepatitis, J. Hepatol. 59 (2013) 563–570.
[32] P. Puri, R.A. Baillie, M.M. Wiest, et al., A lipidomic analysis of nonalcoholic fatty

liver disease, Hepatology 46 (2007) 1081–1090.
[33] N. Miyoshi, L. Iuliano, S. Tomono, et al., Implications of cholesterol autoxidation products in the pathogenesis of inflammatory diseases, Biochem. Biophys. Res. Commun. 446 (2014) 702–708.
[34] J.S. Wooten, H. Wu, J. Raya, et al., The influence of an obesogenic diet on oxysterol metabolism in C57BL/6J mice, Cholesterol 2014 (2014) 843468.
[35] D.M. Van Rooyen, C.Z. Larter, W.G. Haigh, et al., Hepatic free cholesterol accumulates in obese, diabetic mice and causes nonalcoholic steatohepatitis, Gastroenterology 141 (1393–403) (2011) 1403.
[36] L. Xu, Q. Bai, D. Rodriguez-Agudo, et al., Regulation of hepatocyte lipid metabolism and inflammatory response by 25-hydroxycholesterol and 25-hydroxycholesterol-3-sulfate, Lipids 45 (2010) 821–832.
[37] V. Bieghs, T. Hendrikx, P.J. van Gorp, et al., The cholesterol derivative 27-hydroxycholesterol reduces steatohepatitis in mice, Gastroenterology 144 (2013) 167–178.
[38] L. Xu, J.K. Kim, Q. Bai, et al., 5-cholesten-3beta,25-diol 3-sulfate decreases lipid accumulation in diet-induced nonalcoholic fatty liver disease mouse model, Mol. Pharmacol. 83 (2013) 648–658.
[39] M. Deushi, M. Osaka, K. Nakano, et al., Ezetimibe reduced hepatic steatosis induced by dietary oxysterols in nonhuman primates, FEBS Open Bio 6 (2016) 1008–1015.
[40] L. Ryan, Y.C. O'Callaghan, N.M. O'Brien, The role of the mitochondria in apoptosis induced by 7beta-hydroxycholesterol and cholesterol-5beta,6beta-epoxide, Br. J. Nutr. 94 (2005) 519–525.
[41] H. Liu, T. Wang, K. Huang, Cholestane-3beta,5alpha,6beta-triol-induced reactive oxygen species production promotes mitochondrial dysfunction in isolated mice liver mitochondria, Chem. Biol. Interact. 179 (2009) 81–87.
[42] V. Leoni, T. Nury, A. Vejux, et al., Mitochondrial dysfunctions in 7-ketocholesterol-treated 158N oligodendrocytes without or with alpha-tocopherol: impacts on the cellular profil of tricarboxylic cycle-associated organic acids, long chain saturated and unsaturated fatty acids, oxysterols, cholesterol and cholesterol precursors, J. Steroid Biochem. Mol. Biol. (2016).
[43] P. Nordmann, M. Diez-Ibanez, M. Chessebeuf-Padieu, et al., Toxic effects of 7 beta-hydroxycholesterol on rat liver primary cultures, epithelial lines and co-cultures, Cell Biol. Toxicol. 5 (1989) 261–270.
[44] R.A. Schweizer, M. Zurcher, Z. Balazs, et al., Rapid hepatic metabolism of 7-ketocholesterol by 11beta-hydroxysteroid dehydrogenase type 1: species-specific differences between the rat, human, and hamster enzyme, J. Biol. Chem. 279 (2004) 18415–18424.
[45] A. Franko, J.C. von Kleist-Retzow, S. Neschen, et al., Liver adapts mitochondrial function to insulin resistant and diabetic states in mice, J. Hepatol. 60 (2014) 816–823.
[46] A.M. Betancourt, A.L. King, J.L. Fetterman, et al., Mitochondrial-nuclear genome interactions in non-alcoholic fatty liver disease in mice, Biochem. J. 461 (2014) 223–232.
[47] R.C. Scarpulla, Metabolic control of mitochondrial biogenesis through the PGC-1 family regulatory network, Biochim. Biophys. Acta 1813 (2011) 1269–1278.
[48] C. Koliaki, J. Szendroedi, K. Kaul, et al., Adaptation of hepatic mitochondrial function in humans with non-alcoholic fatty liver is lost in steatohepatitis, Cell Metab. 21 (2015) 739–746.